Microwave Ablation: The Differences Between Biliary Cirrhosis and Normal Porcine Liver Using a Cooled-tip Electrode

LI-GANG WANG[1*], WEN-JIN JIANG[1*], WEI-JUN FAN[2], YAN-BO ZHENG[1], XUE-PENG SONG[1], SHENG LIU[1], BO-LIN SUN[1] and TAO WANG[1]

[1]*Department of Medical Imaging & Interventional Radiology, Yu Huang Ding Hospital, Qing Dao University Medical College, Yantai, Shandong, P.R. China;*
[2]*Department of Medical Imaging & Interventional Radiology, Sun Yat-sen University Cancer Center, Guangzhou, Guangdong, P.R. China*

Abstract. *Aim: To elucidate the difference in both in vivo and ex vivo microwave ablation in a biliary cirrhotic porcine liver model using a cooled-tip electrode. Materials and Methods: Microwave ablation with cooled-tip electrode was conducted under laparotomy. Morphological and pathological characteristics of the ablated areas were compared. Results: In the cirrhotic liver group, the in vivo ablated area was smaller than that ex vivo in terms of short and long axes, and volume. With the same ablation settings, both in vivo and ex vivo ablated areas in normal pig liver were larger than their counterparts in cirrhotic liver in terms of the short and long axes, and volume. Conclusion: Both in vivo and ex vivo ablated areas in biliary cirrhotic pig liver were smaller than their counterparts in normal liver, suggesting that for the same amount of power, it requires a significantly longer duration to achieve the same ablated volume in cirrhotic liver compared to normal liver.*

Hepatocellular carcinoma is the sixth most common cancers in the world with more than 700,000 newly, diagnosed cases per year and the third leading cause of cancer-related deaths worldwide (1). In the People's Republic of China, one of the largest hepatitis-endemic countries, the incidence of liver cancer surpasses the world's average and its mortality rate ranks second among malignant neoplasms (2).

*These Authors contributed equally to this study and share first authorship.

Correspondence to: Wei-jun Fan, Ph.D., Department of Medical Imaging & Interventional Radiology, Sun Yat-sen University Cancer Center, Guangzhou, Guangdong, P.R. China. Tel: +86 02087343013, Fax: +86 02087343013, e-mail: fanweijun1964@126.com

Key Words: Microwave ablation, pigs, liver cirrhosis, animal model.

In recent years, there has been substantial progress in image-guided thermal ablation therapies for primary liver cancer, including radiofrequency ablation, microwave ablation, and high-intensity focused ultrasound (3, 4). Although radiofrequency ablation was developed earlier and has been studied more thoroughly than other methods, percutaneous microwave coagulation therapy (PMCT) is rising in importance due to its better thermal efficiency, complete ablation rate, and better long-term therapeutic outcome. However, all animal studies on PMCT, to date, have been conducted using models of normal liver (5-7). We used an animal model of liver cirrhosis using PMCT in order to determine the differences between *in vivo* and *ex vivo* ablation in a cirrhotic *versus* normal porcine liver.

Materials and Methods

Establishment of the biliary cirrhosis model. All experimental animals were supplied by the Center for Laboratory Animal Sciences of the Southern Medical University in Guangzhou, Guangdong, P.R. China. This study was approved by the Research Animal Care and Use Committee (Approval ID: YYYLLS [2012] 83). Six Tibetan miniature pigs, aged 3 months±10 days, weighing 26.7-31 kg (with an average of 28.94 kg) were used. Four underwent common bile duct ligation. Two did not undergo any surgery and were designated as the controls.

No food was allowed for 24 h and no water intake was permitted 12 h before common bile duct ligation. The animals received an intramuscular injection of 1 mg of atropine 30 minutes before surgery. Basal anaesthesia using 0.2-03 g of ketamine and 3-4.5 ml of Su-Mian-Xin (a veterinary anaesthetic comprising xylidinothiazole, dihydroetorphine, and haloperidol) was performed. After fixation under basal anaesthesia, procaine was given *via* drip infusion into the auricular vein, at an adjustable drip rate according to the anaesthetic level. Intramuscular injections of 1-3 ml Su-Mian-Xin were given, as needed.

Under laparotomy, the common bile duct was exposed, double ligated with silk suture, and cut between the ligations. Approximately 30 min after surgery, the animal was able to stand

and walk on its own feet. Brown urine was noted 3-5 days after surgery, suggesting successful common bile duct ligation. Postsurgical haemostatic and anti-inflammatory therapies were given for 3 consecutive days post surgery.

Liver biopsy results in the experimental group. After ligation, the four experimental pigs exhibited reduced appetite, weight loss, and slowed growth. One died on the 14th day after surgery, with a potential cause of death being infection complicated by liver failure. Two months after surgery, the other three pigs with ligated common bile ducts underwent computer tomographic (CT)-guided liver biopsy. With haematoxylin and eosin (H&E) staining, the specimens showed hepatocellular degeneration with abundant cytoplasm. Focal necrosis accompanied by biliary dilation and cholestasis was found. In the portal triads, there was remarkable proliferation of collagen fibre in patches and the formation of pseudo-lobules, suggesting development of typical cirrhosis.

Microwave ablation with cooled-tip electrode. Five pigs were prepared for microwave ablation, including three pigs with pathologically confirmed biliary cirrhosis (the experimental group), and two with normal livers (the control group).

A microwave delivery system with cooled-tip electrode for inter-tissue tumor [power: 5-100 W, frequency: 2,450 MHz, continuous adjustable time range: 1-99 min; MTC-3 (C); Qinghai Microwave Electronic Institute, Nanjing, China] was used. The device was equipped with a water-cooled antenna, 15 cm in length and 1.9 mm in diameter, with high-power capacity that was suitable for direct use in percutaneous puncture. A peristaltic pump (BT01-100; Longer Precision Pump, Baoding, China) was used to drive the cooling water circlating in the microwave antenna. A bottle of 500-ml sterile normal saline solution at room temperature served as the cooling source as water passed through the closed system composed of pipes and the antenna. According to our experience, microwave ablation therapy with the power set at 70 W has generally been adapted to clinical settings. Therefore, the ablation setting used was 70 W of power for a duration of 5 min.

The five pigs were divided into four groups: Group 1, *in vivo* ablation on normal liver of two pigs; group 2, *ex vivo* ablation on normal liver of two pigs(the same two as group 1); group 3, *in vivo* ablation on cirrhotic liver of three pigs; and group 4, *ex vivo* ablation on cirrhotic liver of three pigs(the same three as group 3).

Laparotomy was performed through layer-by-layer incision to expose the liver. Upon gross inspection, the cirrhotic liver appeared smaller in volume, dark-yellow in colour, with numerous nodules of various sizes on its surface, and was slightly firm in texture. It was accompanied by a notably enlarged gall bladder. Mild ascites in the abdominal cavity and intrahepatic cholangiectasis were noted in one of the pigs (Figure 1).

Microwave ablation was performed at 4-5 sites for each liver. Since the right posterior lobe of the pig liver is located deep in the abdominal cavity where it is difficult to reach, it served as the *ex vivo* ablation site. Two to three other sites were selected to perform *in vivo* ablation.

The microwave ablation system was connected according to the manual, the ablation power was set at 70 W and the duration of ablation was set at 5 mins. The microwave ablation needle was inserted 5-6 cm into the liver under direct observation. After the ablation, the animal was sacrificed with a lethal dose of intravenous ketamine. After removal of the liver, *ex vivo* ablation was performed at its right posterior lobe. A total of 23 ablation sites were used in this study with 5, 4, 8, and 6 sites in the four groups, respectively.

Table I. *Measurements of ablation areas in the various groups (mean±SD; n=23)*

Group	Short axis (cm)	Long axis (cm)	Volume (cm^3)
1	2.04±0.05	3.14±0.11	6.85±0.46
2	2.30±0.18	3.60±0.08	10.03±1.73
3	1.90±0.10	2.95±0.12	5.97±0.75
4	2.08±0.08	3.08±0.75	7.01±0.47

Group 1, *In vivo* ablation on normal liver; group 2, *ex vivo* ablation on normal liver; group 3, *in vivo* ablation on cirrhotic liver; and group 4, *ex vivo* ablation on cirrhotic liver.

Upon completion of the ablation, all of the ablated specimens were dissected horizontally along the direction of the microwave antenna. Upon gross inspection, the ablated area, peripheral congestion zone, and the hepatic parenchymal zone were identified. The longitudinal lengths of the ablated area and the congestion zone, in the shape of an ellipsoid of which the long axis was along the needle track, were measured. The length of the short axis, the widest span perpendicular to the long axis, was also measured.
The ablation volume was calculated using the ellipsoid volume formula:

$V=\pi xyz/6$ (8, 9), where x: the longitudinal axis; $y=z$, the cross axis; V: the ablation volume.

Pathological section and staining. The tissues at and around the ablation site were removed and fixed in 10% formaldehyde. Pathological slides, prepared after paraffin embedding, sectioning, and H&E staining, were then examined.

Statistical analysis. SPSS 13.0 statistical software was used (SPSS Inc., Chicago, IL, USA), and the results were shown as mean±SD. Paired comparison among the four groups were conducted using t-test. A p-value of less than 0.05 was considered statistically significant.

Results

Morphology and characteristics of ablation sites. In cross-section along the long axis, all ablation sites appeared oval, with clear borders separating them from the surrounding normal liver tissue. Upon gross inspection, the site consisted of four zones. The first zone, the central carbonization zone, was a cone-shaped area appearing on the sides and at the tip of the antenna. In groups 1 and 2 (representing ablation of normal liver), this zone was prominent, with an average diameter of 4.2 mm, whereas in groups 3 and 4 (representing ablation in biliary cirrhotic liver), the zone was smaller, with an average diameter of 2.6 mm.

The second zone was of coagulated necrosis, which was an oval-shaped area surrounding the carbonization zone and also the largest of the four zones. As a zone of heat-

Table II. *Paired comparisons of the measurements among groups (p-value).*

Parameter	Group 1 *vs*. 2	Group 1 *vs*. 3	Group 2 *vs*. 4	Group 3 *vs*. 4
Short axis	0.06	0.11	0.09	0.028
Long axis	<0.001	0.019	<0.001	0.026
Volume	0.031	0.024	0.036	0.008

Group 1, *In vivo* ablation on normal liver; group 2, *ex vivo* ablation on normal liver; group 3, *in vivo* ablation on cirrhotic liver; and group 4, *ex vivo* ablation on cirrhotic liver.

coagulated necrosis, it appeared gray-white in groups 1 and 2, and dark yellow or golden in groups 3 and 4.

The third zone was that of congestion and oedema, located between the zone necrosis and liver parenchyma. The zone appeared pink in groups 1 and 2, and dark yellow in groups 3 and 4.

The fourth zone, or liver parenchymal zone, surrounded the zone of congestion and oedema. In groups 1 and 2, the normal liver parenchyma appeared dark red with tender texture, whereas in groups 3 and 4, it appeared dark brown with firm texture, and the surface of the liver parenchyma was nodular (Figure 2).

Comparisons of measurements of the ablation areas. The data in Tables I and II show that normal liver had *in vivo* ablated areas that were smaller than *ex vivo* ablated areas in terms of the short and long axes, and volume. There were statistically significant differences in the long axis and volume ($p<0.001$ and $p=0.031$, respectively), whereas the difference in the short axis failed to reach statistical significance ($p=0.06$).

In our porcine model of liver cirrhosis, *in vivo* ablated areas were smaller than *ex vivo* ablated areas in terms of short and long axes, and volume, and all differences reached statistical significance ($p=0.028$, $p=0.026$, and $p=0.008$, respectively). Under the same ablation settings, both *in vivo* and *ex vivo* ablated sites in normal liver were larger than their counterparts in cirrhotic liver in terms of short and long axes, and volume. There were significant differences in the long axis and volume ($p=0.019$, $p=0.00$, $p=0.024$, and $p=0.036$, respectively), while the differences in the short axis between *in vivo* and *ex vivo* ablated areas failed to reach statistical significance ($p=0.11$ and $p=0.09$).

Pathological examination of ablated areas. Upon H&E staining, in the central carbonization zone, there was significant hepatocellular damage, ruptured and fissured hepatic plates, and indistinguishable hepatocellular structure with condensed cellular nuclei. In the zone of coagulated necrosis, there were incomplete and distorted cell plates in some cells. In addition, mildly swollen hepatocytes without other significant morphological changes were present. Sporadic necrotic cells were also seen in that area. In the cirrhotic liver, intrahepatic cholestasis without major morphological changes from normal liver parenchyma was noted. Regarding congestion and oedema, there were intact hepatic plates and no significant changes in hepatocellular structures were noted. The liver parenchymal zone was described earlier (see Liver biopsy results in the experimental group) (Figure 3).

Discussion

Percutaneous ablation therapies are novel, minimally invasive tumor therapies that have become increasingly popular in the past decade. Among the most commonly used ones in the clinical setting, radiofrequency and microwave ablation therapies have shown favourable therapeutic effects on liver cancer with comparable outcomes to that of surgery, in some cases (10, 11). In recent years, animal and clinical studies on radiofrequency and microwave ablation therapies have become a focused area of interventional research. Despite its more recent development, microwave ablation is preferred by several researchers (12-15) because it is less influenced by the 'heat-sink' effects of blood vessels and is less influenced by the electric conductivity of the surrounding tissue. In addition, its fast and broad heating with high intra-tumor temperature facilitates fast ablation over a larger therapeutic area. It is also free of electrode-related complications such as tissue burn.

In recent years, PMCT has been developed as a new therapeutic technique for liver cancer. In light of microwave thermal effects coupled with the heat-sensitive characteristics of neoplasms, PMCT achieves *in situ* ablation of cancer cells through application of local heat at 60-107˚C in a short time, resulting in tissue necrosis. Since 1994, when Seki *et al*. first reported the use of PMCT to treat small hepatocellular carcinoma (16), the technique has gained wide application. PMCT achieves its therapeutic effect *via* an alternating electric field generated by microwave radiation. Heat is created by collision and friction of massive numbers of charged particles such as potassium, sodium and chloride, and polar molecules such as water and proteins, in both intra- and extracellular fluid. Upon reaching a temperature

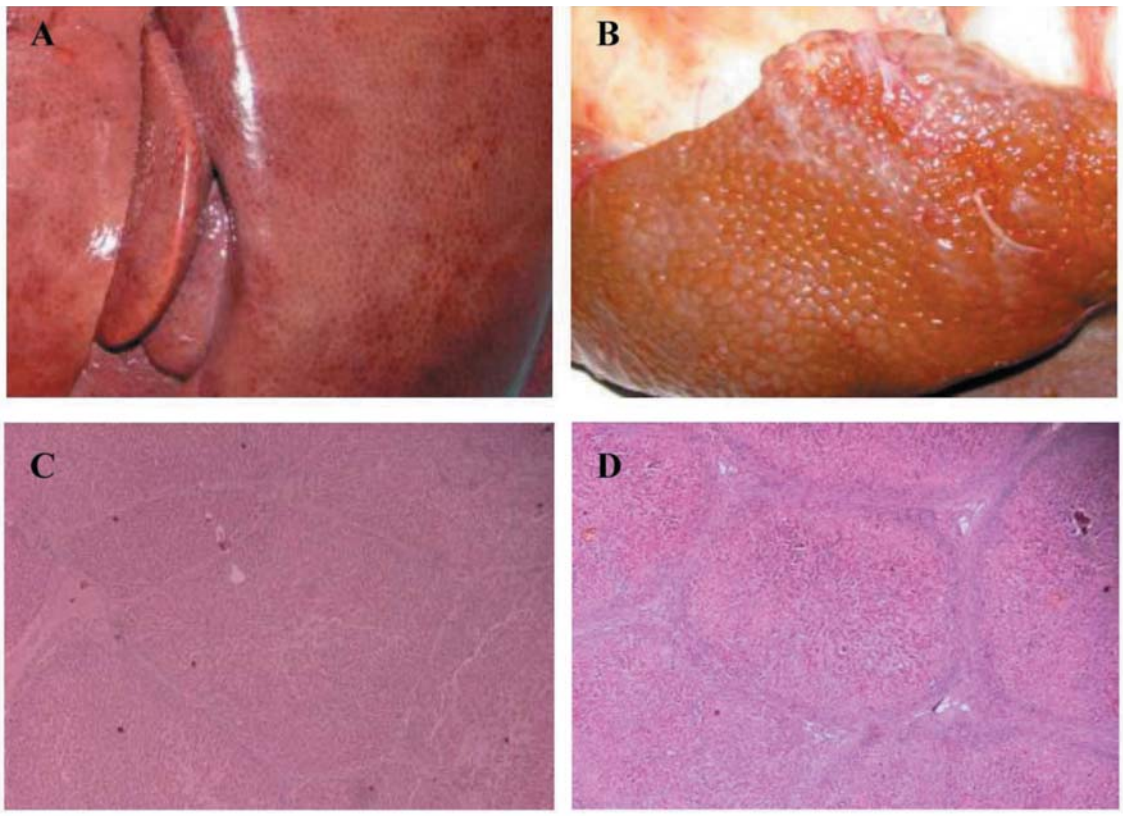

Figure 1. *Histological assessment. A: Normal pig liver with dark red colour, smooth surface and tender texture. B: Liver of a pig with biliary cirrhosis, with dark yellow colour, nodular surface and firm texture. C: Normal pig liver, H&E staining: intact hepatic plates, clear lobular structure (×40). D: Liver of a pig with biliary cirrhosis, H&E staining: significant fibrosis in patches, with visible 'pseudo-lobules' (×40).*

of 54˚C or more, protein coagulation results in irreversible cellular damage (17). Because PMCT delivers microwave radiation through needle-like electrodes, it produces highly concentrated therapeutic heat that can completely destroy all tissues in the target area while ensuring the safety of the surrounding tissues.

After ablation, tumor tissues release heat-shock proteins that stimulate the body's immune system, and the enhanced local and systemic immunity may limit the spread of tumour cells. It has been shown that after PMCT, the number of immunocytes in the tumour and the surrounding liver tissues increases significantly, suggesting activation of local immunological functions (17). Complete *in situ* ablation of the tumour is the key to increased local infiltration of immunocytes following therapy (18). Therefore, the ability to eliminate both the tumour and the remaining cancer cells and to prevent recurrence may account for favorable long-term outcomes of PMCT and lower recurrence rates (19). To date, all animal studies on microwave ablation have been conducted in normal healthy animal liver models (5, 6, 8, 9). We are among the few to have conducted microwave ablation using an animal model of liver cirrhosis. Due to the anatomical similarity between pigs and humans in terms of liver structure, texture, and vascular distribution, pigs were used in this study as the experimental animal.

Currently there are a number of methods for establishing a porcine model of liver cirrhosis. The most common ones include dimethylnitrosamine induction of cirrhosis, alcoholic cirrhosis model, carbon tetrachloride induction of cirrhosis, and the biliary cirrhosis model. The latter was adopted in this study because of its relatively simple procedures, little contamination, and short model construction time.

Two months after double ligation of the common bile duct, three out of the four Tibetan miniature pigs were pathologically diagnosed with liver cirrhosis by liver biopsy, while the remaining pig died of infection complicated by liver failure 14 days after surgery. The procedure achieved a 100% formation rate of liver cirrhosis. Given that liver cancer usually develops from liver cirrhosis, we conducted this study on microwave ablation in a pig liver model of biliary cirrhosis in order to determine whether the ablated area in a cirrhotic liver equals that in normal liver under the same ablation settings.

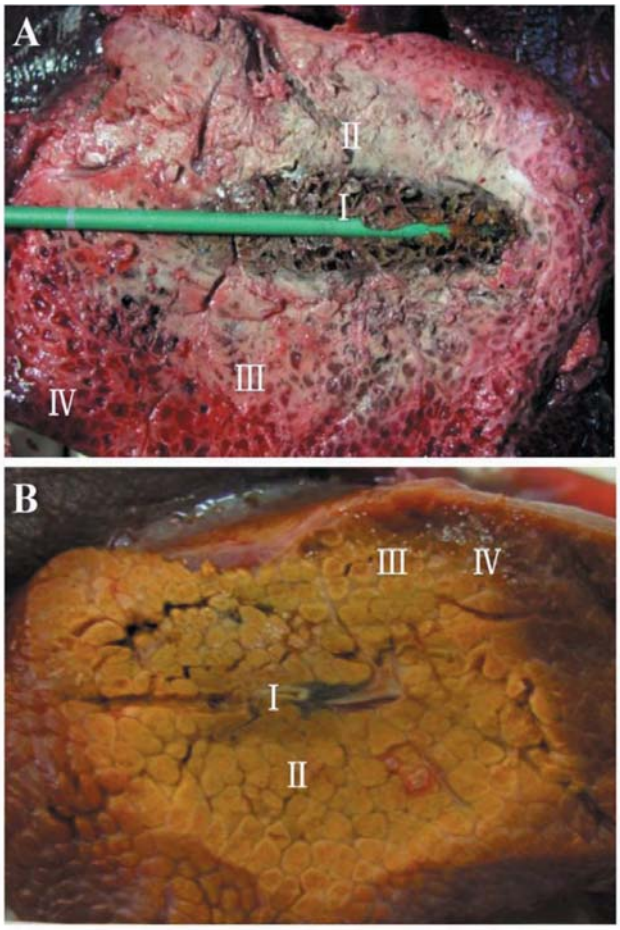

Figure 2. *Assessment of ablation. A: Cross section of normal pig liver after ablation shows zones of carbonization (I), coagulated necrosis (II), congestion (III), and liver parenchymal zone (IV), clearly bordering each other. B: Cross section of liver from a pig with biliary cirrhosis after ablation shows the same distribution of the four zones as in normal liver, but with a smaller carbonization zone with remarkably different colouration.*

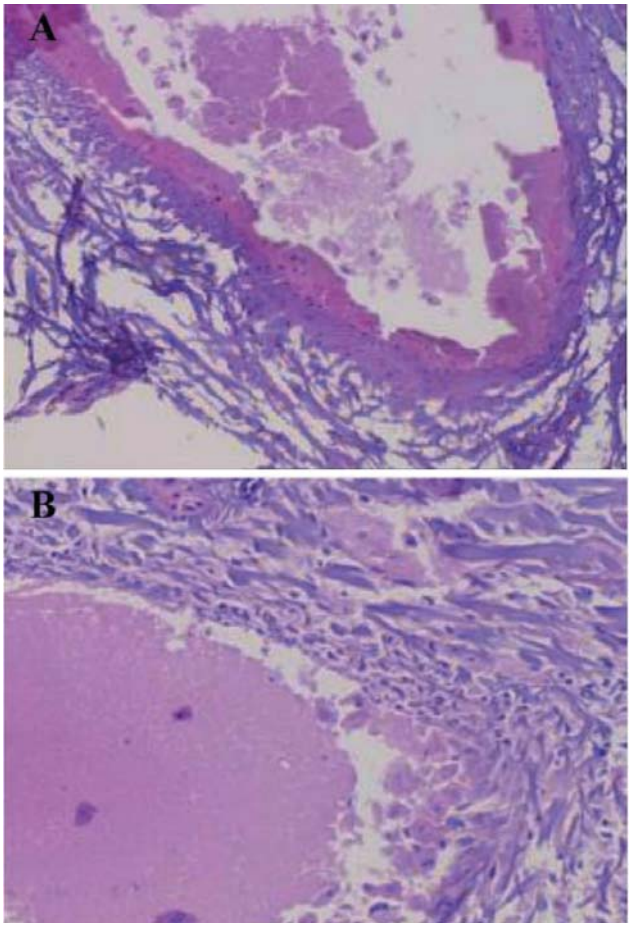

Figure 3. *Histological assessment of liver tissues after ablation in normal pig liver (A) and liver of a pig with biliary cirrhosis (B). H&E staining shows broken and severed hepatic plates with visible zones of carbonization and necrosis, ×100.*

After ablation at 70 W for 5 min, the short and long axes and volume of *in vivo* ablated areas were 1.90±0.10 cm, 2.95±0.12 cm, and 5.97±0.75 cm^3 compared to 2.08±0.08 cm, 3.08±0.75 cm, and 7.01±0.47 cm^3 of areas under *ex vivo* ablation. These results suggest that under the same ablation settings, *in vivo* ablation affected a smaller area than did *ex vivo* ablation, in line with previous animal studies. This may be related to the 'heat-sink' phenomenon by which heat is carried away during the *in vivo* procedure reducing the actual energy within the target area. Such an explanation has been accepted by many researchers (20-22).

One of our more interesting findings was the significantly smaller *in vivo* and *ex vivo* ablation areas in cirrhotic liver compared to normal liver under the same ablation settings. The mechanism underlying microwave ablation involves the generation of an electromagnetic field that oscillates water, charged particles and polar molecules around the tissue, creating friction and heat that is lethal to cells. We believe that in a cirrhotic liver, the hepatocellular degeneration and necrosis decrease thermal conductivity, and the significant overgrowth of fibrotic tissue (that also exhibits poorer thermal conductivity) acts like a natural barrier to heat, resulting in a smaller ablated area (23, 24). Our findings suggest that for the same amount of power, it requires a significantly longer time to achieve the same ablated volume in cirrhotic liver compared to normal liver. Different degrees of cirrhosis may be translated into different areas of ablation. Therefore, in the clinical setting, the optimal ablation criteria require the adoption of different reference points according to the degree of cirrhosis. For patients with more advanced cirrhosis and more significant fibrosis, the ablation time should be relatively prolonged in order to prevent incomplete ablation and residual tumor.

Our study had several limitations. We used a biliary cirrhosis model, however, most clinical cases of liver cancer originate from portal cirrhosis caused by hepatitis B or C or from alcoholic cirrhosis. In addition, the number of experimental animals was small, and only one ablation setting using a power of 70 W and a duration of 5 min was used as the observation point, while other settings were not tested. Considering that this is only a preliminary study, future studies should include a larger sample size and increased number of observation points.

Conclusion

For patients with more advanced cirrhosis and more significant fibrosis, the ablation time should be relatively prolonged in order to prevent incomplete ablation with viable residual tumor.

References

1 Jemal A, Bray F, Center MM, Ferlay J, Ward E and Forman D: Global cancer statistics. CA Cancer J Clin *61*: 69-90, 2011.

2 He J, Gu D, Wu X, Reynolds K, Duan X, Yao C, Wang J, Chen CS, Chen J, Wildman RP, Klaq MJ and Whelton PK: Major causes of death among men and women in china. N Engl J Med *353*: 1124-1134, 2005.

3 Li D, Kang J, Golas BJ, Yeung VW and Madoff DC: Minimally invasive local therapies for liver cancer. Cancer Biol Med *11*: 217-236, 2014.

4 Yu H and Burke CT: Comparison of percutaneous ablation technologies in the treatment of malignant liver tumors. Semin Intervent Radiol *31*: 129-137, 2014.

5 Andreano A, Huang Y, Meloni MF, Lee FT Jr. and Brace C: Microwaves create larger ablations than radiofrequency when controlled for power in *ex vivo* tissue. Med Phys *37*: 2967-2973, 2010.

6 Ha EJ, Baek JH and Lee JH: Moving-shot *versus* fixed electrode techniques for radiofrequency ablation: comparison in an *ex vivo* bovine liver tissue model. Korean J Radiol *15*: 836-843, 2014.

7 Harari CMMagagna M, Bedoya M, Lee FT Jr, Lubner MG, Hinshaw JL, Ziemlewicz T and Brace CL: Microwave ablation: comparison of simultaneous and sequential activation of multiple antennas in liver model systems. Radiology *278*: 95-103, 2016.

8 Burdio F, Navarro A, Berjano EJ, Burdio JM, Gonzalez A, Güemes A, Sousa R, Rufas M, Crruz I, Castiella T, Lozano R, Lquerica JL and Grande L: Radiofrequency hepatic ablation with internally cooled electrodes and hybrid applicators with distant saline infusion using an *in vivo* porcine model. Eur J Surg Oncol *34*: 822-830, 2008.

9 Lee JM, Han JK, Kim HC, Choi YH, Kim SH, Choi JY and Choi Bl: Switching monopolar radiofrequency ablation technique using multiple, internally cooled electrodes and a multichannel generator: *ex vivo* and *in vivo* pilot study. Invest Radiol *42*: 163-171, 2007.

10 Dong B, Liang P, Yu X, Su L, Yu D, Cheng Z and Zhang J: Percutaneous sonographically guided microwave coagulation therapy for hepatocellular carcinoma: results in 234 patients. AJR Am J Roentgenol *180*: 1547-1555, 2003.

11 Wong KM, Yeh ML, Chuang SC, Wang LY, Lin ZY, Chen SC, Tsai JF, Wang SN, Kuo KK, Dai CY, Yu ML, Lee KT and Chuang WL: Survival comparison between surgical resection and percutaneous radiofrequency ablation for patients in Barcelona Clinic Liver Cancer early-stage hepatocellular carcinoma. Indian J Gastroenterol *32*: 253-257, 2013.

12 Simon CJ, Dupuy DE and Mayo-Smith WW: Microwave ablation: principles and applications. Radiographics *25*: S69-83,2005.

13 Brace CL: Microwave ablation technology: What every user should know. Curr Probl Diagn Radiol *38*: 61-67, 2009.

14 Huo YR and Eslick GD: Microwave ablation compared to radiofrequency ablation for hepatic lesions: a meta-analysis. J Vasc Interv Radiol *26*: 1139-1146, 2015.

15 Poulou LS, Botsa E, Thanou I, Ziakas PD and Thanos L: Percutaneous microwave ablation *vs*. radiofrequency ablation in the treatment of hepatocellular carcinoma. World J Hepatol *7*: 1054-1063, 2015.

16 Seki T, Wakabayashi M, Nakagawa T, Itho T, Kunieda K, Sato M, Uchiyama S and Inoue K: Ultrasonically guided percutaneous microwave coagulation therapy for small hepatocellular carcinoma. Cancer *74*: 817-825, 1994.

17 Dong BW, Zhang J, Liang P, Yu XL, Su L, Yu DJ, Ji XL and Yu G: Sequential pathological and immunologic analysis of percutaneous microwave coagulation therapy of hepatocellular carcinoma. Int J Hyperthermia *19*: 119-133, 2003.

18 Gressner AM: Transdifferentiation of hepatic stellate cells (Ito cells) to myofibroblasts: a key event in hepatic fibrogenesis. Kidney Int Suppl *54*: S39-45, 1996.

19 Chou WY, Lu CN, Lee TH, Wu CL, Hung KS, Concejero AM, Jawan B and Wang CH: Electroporative interleukin-10 gene transfer ameliorates carbon tetrachloride-induced murine liver fibrosis by MMP and TIMP modulation. Acta Pharmacol Sin *27*: 469-476, 2006.

20 Yu J, Liang P, Yu X, Liu F, Chen L and Wang Y: A comparison of microwave ablation and bipolar radiofrequency ablation both with an internally cooled probe: Results in *ex vivo* and *in vivo* porcine livers. Eur J Radiol *79*: 124-130, 2011.

21 Wright AS, Sampson LA, Warner TF, Mahvi DM and Lee FT Jr.: Radiofrequency *versus* microwave ablation in a hepatic porcine model. Radiology *236*: 132-139, 2005.

22 Pillai K, Akhter J, Chua TC, Shehata M, Alzahrani N, Al-Alem I and Morris DL: Heat-sink effect on tumor ablation characteristics as observed in monopolar radiofrequency, bipolar radiofrequency, and microwave, using *ex vivo* calf liver model. Medicine *94*: e580, 2015.

23 Meloni MF, Goldberg SN, Moser V, Piazza G and Livraghi T: Colonic perforation and abscess following radiofrequency ablation treatment of hepatoma. Eur J Ultrasound *15*: 73-76, 2002.

24 Livraghi T, Goldberg SN, Lazzaroni S, Meloni F, Ierace T, Solbiati L and Gazelle GS: Hepatocellular carcinoma: radiofrequency ablation of medium and large lesions. Radiology *214*: 761-768, 2000.

Received January 18, 2016
Revised February 22, 2016
Accepted February 23, 2016